

Diffuse cliques maintain biodiversity in species-rich ecological communities

Matthieu Barbier^{1,3*}, Claire de Mazancourt¹, Michel Loreau¹ and Guy Bunin²

May 28, 2019

1 **High-dimensional phenomena, which often defy
2 low-dimensional intuitions^{1;2}, are an essential and
3 yet seldom explored frontier in our understanding
4 of ecological communities³. Ecologists have long
5 speculated about how large numbers of species
6 manage to coexist in rich assemblages. Most an-
7 swers to date have focused on identifying partic-
8 ular dimensions along which species may orga-
9 nize to persist together⁴. Here we instead ask:
10 what is the characteristic structure of a commu-
11 nity where coexistence arises from a large num-
12 ber of concurrent factors? In such communities,
13 individual species might not follow any evident
14 pattern in their interactions, yet the group as a
15 whole exhibits a statistical structure that we call
16 “diffuse clique”. We find remarkable quantita-
17 tive evidence for this pattern across a range of
18 plant biodiversity experiments. Our approach ex-
19 ploits the emergent simplicity of high-dimensional
20 systems^{5;6}, a powerful idea originating in physics
21 that has, so far, rarely been demonstrated un-
22 equivocally in ecological data. We conclude that a
23 subtle form of collective order may underlie com-
24 plex networks of species interactions. This diffuse
25 order offers a new grasp on how ecological com-
26 munities maintain their fascinating diversity.**

27 The coexistence of many species with similar attributes
28 is a long-standing puzzle: simple theories and exper-
29 iments support the principle of competitive exclusion,
30 whereby the best competitor should displace all others^{7;8}.
31 Yet, strict dominance by one species appears, at most
32 spatial and temporal scales, to be the exception rather
33 than the rule in the natural world. Over decades of
34 ecological research, many partial solutions to this puz-
35 zle have been proposed, and integrated into the overar-

ching framework of niche theory⁹. This framework sug-
36 gests that we should identify particular trade-offs between
37 abilities such as resource exploitation¹⁰, defense against
38 predators¹¹ and tolerance of temporal fluctuations^{12;13}.
39 Through these trade-offs, strict bounds are imposed upon
40 how species grow and interact, preventing any species
41 from overwhelming its competitors.

42 We propose to start from a different perspective. Co-
43 existence in highly diverse communities likely involves a
44 large number of niches and trade-offs, some known and
45 many unknown *a priori*¹⁴. Each cross-species interaction
46 may be determined by a unique combination of factors,
47 precluding any simple and conspicuous (low-dimensional)
48 order in the community³. Some ecological theories there-
49 fore make the assumption that interactions are essentially
50 random⁵ – a bold move, yet one that parallels major suc-
51 cesses in physics^{15;16}. Fully random interactions, how-
52 ever, do not allow many species to coexist¹⁷. The high
53 biodiversity observed in many natural communities there-
54 fore implies some form of latent structure.

55 We first derive a theoretical prediction, the most par-
56 simonious way to constrain species interactions in order
57 to achieve coexistence. We uncover it by asking: if one
58 samples many different interaction networks, and retains
59 only those where all species survive, what do the remain-
60 ing networks have in common? Some may appear very
61 structured, others almost random. Yet, we find in Fig. 1
62 that *most* of these networks exhibit the same statistical
63 pattern. This pattern, expressed in equations below, is a
64 weak but crucial bias in how the most successful competi-
65 tors interact with others²⁰. We now derive this pattern
66 from a simpler probabilistic argument, and explain in in-
67 tuitive terms how it allows coexistence.

68 Measuring species interactions is often difficult and
69 prone to high uncertainty^{21–23}, and most empirical set-
70 tings only give us access to aggregated statistics. The to-
71 tal effect of interactions on one species i can be inferred
72 from its *relative yield*

$$\eta_i = B_i / K_i \quad (1)$$

73 the ratio of its abundance B_i in a community to its abun-

* Corresponding author: contact@mrcbarbier.org.

¹ Centre for Biodiversity Theory and Modelling, Theoretical and Experimental Ecology Station, UMR 5321, CNRS and Paul Sabatier University, 09200 Moulis, France. ² Department of Physics, Technion-Israel Institute of Technology, Haifa, 3200003 Israel. ³ Institut Natura e Teoria Pirenèus, 75015 Paris, France.

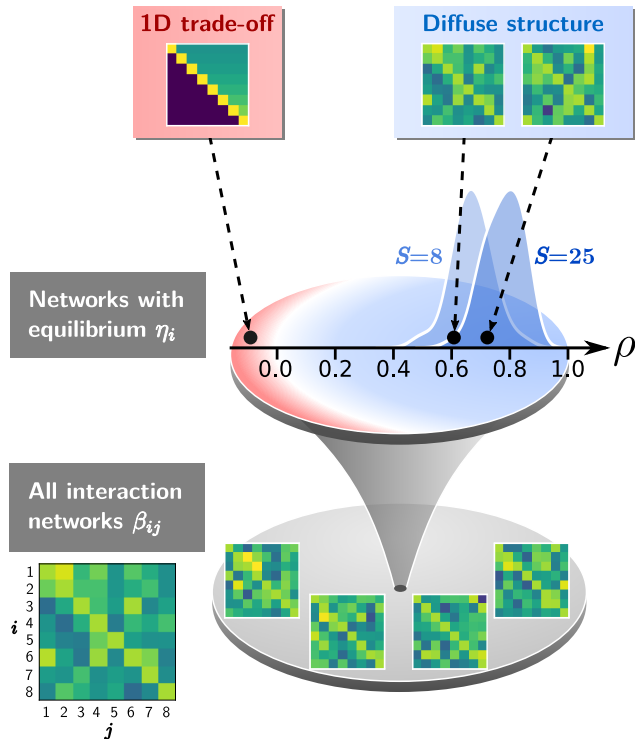


Figure 1: Finding a general pattern of coexistence in species-rich interaction networks. Interaction networks of S species are represented by $S \times S$ matrices (square boxes) where each element β_{ij} denotes the effect of species j on species i . Of all possible species interaction networks (bottom disk), only an infinitesimal fraction (shaded area) allows S species to coexist at some equilibrium η_i . Zooming into this area of coexistence (upper disk), we find that most such networks appear almost random, yet they tend to follow a common trend which we call a “diffuse clique structure”: an underlying pattern of biases (4) and correlations (6) hidden in the large spread of coefficients β_{ij} . We define a metric ρ to quantify how well our predicted pattern is observed in a given interaction network. We find in simulations that this metric ρ gets closer to 1 as biodiversity increases (histograms show the distribution of ρ for 200 networks with $S = 8$ and 25 species). By contrast, some coexistence mechanisms, such as the one-dimensional competition-colonization tradeoff^{18,19}, can give rise to highly atypical networks, showing unrelated or even opposite patterns.

75
76
77
78
79
80
dance without competitors K_i (known as carrying capacity) in the same environment⁹. We interpret species with higher η as *successful* competitors, as they benefit more (or suffer less) in total from their interactions with others. The simplest way to model these interactions is by assuming a linear dependence between species

$$\eta_i = 1 - \sum_{j \neq i} \beta_{ij} \eta_j \quad \text{for all } i. \quad (2)$$

81
82
83
84
85
86
87
88
89
where β_{ij} is the competitive effect of species j on species i . This relationship, which can be tested empirically^{24,25}, holds between coexisting species at equilibrium in the classic Lotka-Volterra model.

90
91
92
93
94
95
96
97
98
99
Many different interaction networks can generate the same equilibrium community. Observing the coexistence of S species with relative yields η_i conveys some information about their interactions, but not enough to fully determine them: the equations (2) impose S constraints, while there are $S(S - 1)$ unknown interaction coefficients β_{ij} . On the other hand, community-wide statistics, such as the mean strength of competition $\bar{\beta}$, can be reliably deduced from that information²⁶ (Appendix E).

100
101
102
103
104
105
106
107
108
109
110
111
We therefore adopt a probabilistic approach, and ask what is the *most likely* community structure, i.e. the set of features most widely shared among the many possible solutions. We first define a prior distribution $P(\beta_{ij})$ that can be adapted to our biological knowledge of the community. For all experiments below, we simply assume that each coefficient β_{ij} is drawn independently from a normal distribution with mean $\bar{\beta}$. We then compute how this prior is modified once restricted to networks that admit the equilibrium η_i (Appendix B). Computing a posterior distribution given a prior and linear constraints (2) is a well-established problem in probability theory^{27,28}.

112
113
114
115
We find that interactions β_{ij} should follow two statistical patterns that both admit intuitive interpretations (Fig. 2). First, competition must be biased to explain which species are successful or not. If all interaction strengths were equal to the prior mean, $\beta_{ij} = \bar{\beta}$, we would expect any species to achieve the same relative yield,

$$\eta^* = \frac{1 - \bar{\beta} \sum_i \eta_i}{1 - \bar{\beta}}. \quad (3)$$

When $\eta_i > \eta^*$, we therefore expect that species i suffers less competition than $\bar{\beta}$, and conversely if $\eta_i < \eta^*$. In our calculation, this appears in the conditional expectation of the competitive effect of j on i ,

$$E[\beta_{ij} | \eta_i, \eta_j] = \bar{\beta} + (1 - \bar{\beta}) \Delta(\eta_i, \eta_j) \quad (4)$$

which deviates from the prior mean $\bar{\beta}$ by a bias

$$\Delta(\eta_i, \eta_j) = -\frac{(\eta_i - \eta^*) \eta_j}{\sum_{m \neq i} \eta_m^2}. \quad (5)$$

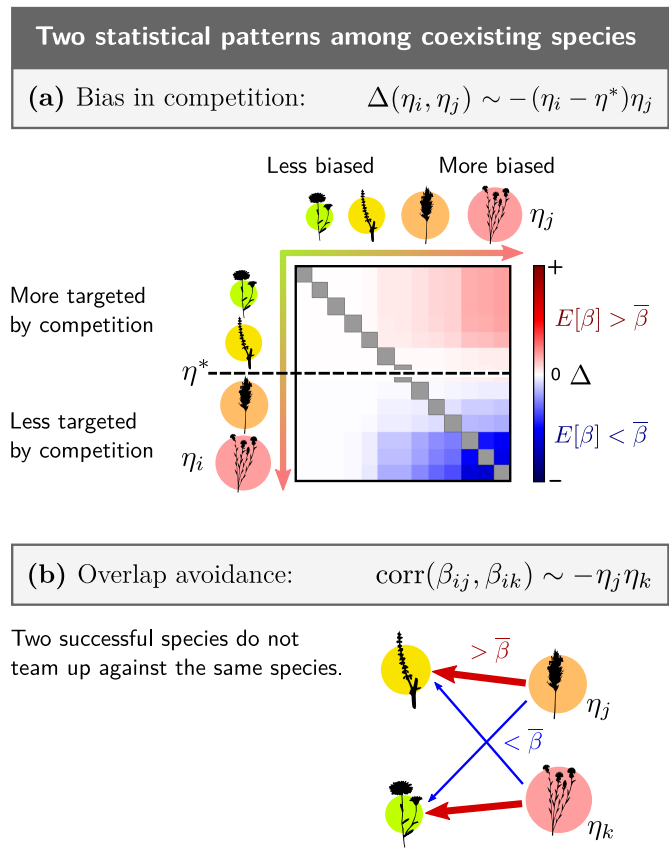


Figure 2: The diffuse clique structure is characterized by two statistical patterns in the competition of successful species. (a) Bias in competitive effects (4). If all species competed with equal strength $\bar{\beta}$, we would expect any given species i to achieve the relative yield $\eta_i = \eta^*$ (3). When η_i differs from this baseline, we can infer how interactions most likely deviate from $\bar{\beta}$. We show this deviation $\Delta(\eta_i, \eta_j)$ for simulated data, in the form of a matrix which we now describe. **Left to right:** a species with low η_j competes indiscriminately against others (white, $\Delta = 0$), whereas a species with high η_j is a biased competitor. **Top to bottom:** species with $\eta_i < \eta^*$ experience stronger competition on average (red, $\Delta > 0$) whereas species with $\eta_i > \eta^*$ experience weaker competition (blue, $\Delta < 0$). Together, these biases indicate the existence of a “clique” of species that compete less against each other, and more against all others, thus achieving higher relative yield than the baseline η^* . (b) Correlation structure between columns of the interaction matrix: the competitive effects of two successful species are anti-correlated, avoiding overlap in which species they affect, whereas competition from unsuccessful species is again indiscriminate.

We see that this bias is not evenly distributed. Competition coming from unsuccessful species (low η_j) can be random without compromising the equilibrium. On the other hand, a species that is successful (achieving high η_j) is likely to have biased interactions, competing less on average against other successful species, and experiencing weaker competition from them (Fig. 2a).

The second pattern imposes that successful species j and k avoid competing against the same target i (Fig. 2b)

$$\text{corr}(\beta_{ij}, \beta_{ik} | \eta_i, \eta_j, \eta_k) = -\frac{\eta_j \eta_k}{\sum_{m \neq i} \eta_m^2}. \quad (6)$$

While the first pattern (4) determines the *expected* success of each species, the second pattern guarantees that each relative yield is *exactly* set to η_i . We show in Appendix B that this correlation pattern prevents η_i from deviating from its expectation, which would likely drive some low- η species to extinction in a fully random community.

Taken together, these two patterns suggest that we will generally observe a fuzzy “clique” of competitors that are both biased and successful, surrounded by unsuccessful species with arbitrary interactions. This picture differs in multiple respects from classic explanations of coexistence. It does not suppose a measurable segregation of species into distinct niches. By imposing only the weakest possible constraints upon the many degrees of freedom in β_{ij} , it allows interactions to take almost arbitrary values. It also represents a form of collective organization, where coexistence arises, not from particular species traits, but from statistical biases distributed over all interactions. Accordingly, Fig. 1 shows that this structure becomes increasingly prevalent (although more diffuse) in highly diverse communities.

We now present an empirical validation of these patterns on experimental data in Fig. 3 and Fig. 4. Grassland biodiversity experiments^{29–31} provide an ideal testbed for inferring species interactions and mechanisms of coexistence. Each experiment contains a large number of plots in which plant species are assembled in varying numbers and combinations, out of a pool of $S = 8$ to 60 species depending on the experiment. Biomass in monoculture (single-species plots) provides an estimate of the species’ carrying capacities.

To test our predictions, we split these data in two sets. Relative yields η_i in the full-diversity plots are used to compute the theoretical expectations (4) and correlations (6) of interactions. All other plots, comprising different subsets of the species pool, are used to fit individual interaction coefficients β_{ij} by a multilinear regression of equation (2). From these fitted coefficients, we construct empirical estimates of the theoretical statistics.

We show in Fig. 3 the interaction matrix computed in the Wageningen grassland experiment. While lacking ap-

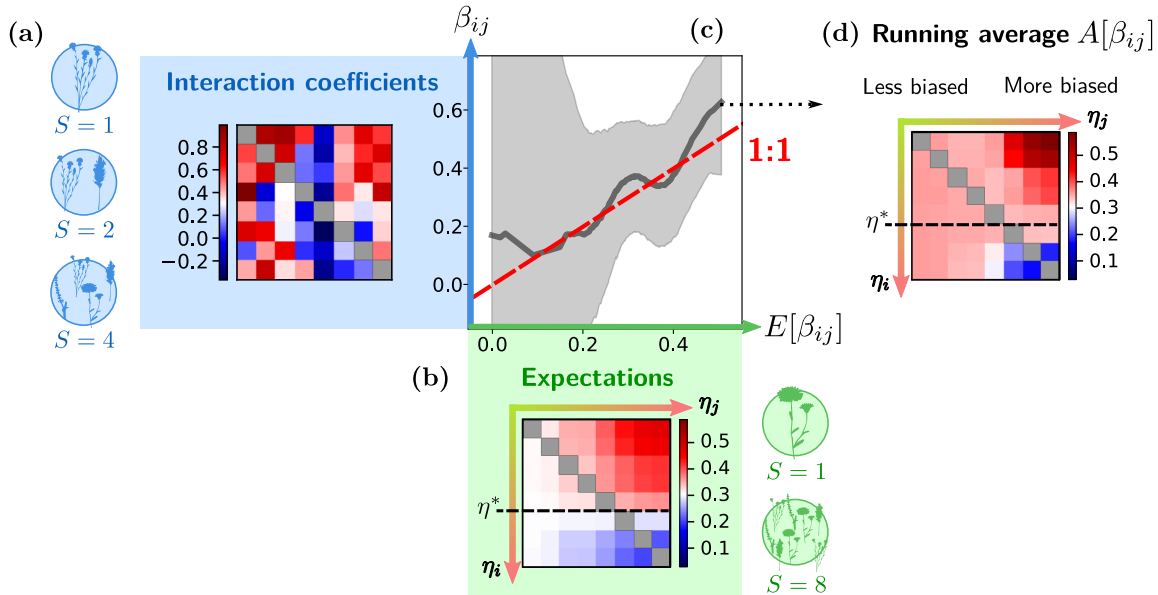


Figure 3: **Diffuse clique in the Wageningen grassland experiment.** (a) Using many species combinations (56 sets of $S < 8$ species), we can fit interaction coefficients β_{ij} by multilinear regression²³. (b) Knowing only the relative yields η_i in the full community (all $S = 8$ species), our method (4) suggests a theoretical expectation for each interaction, $E[\beta_{ij}|\eta_i, \eta_j]$. (c) Comparison between fitted coefficients and expectations. In our diffuse pattern, individual coefficients are expected to exhibit a large spread around their expectation $E[\beta_{ij}]$. But we can construct an empirical estimate of the mean, the running average $A[\beta_{ij}]$ (grey curve, 90% CI in shaded area). It is in good agreement with the theoretical mean, as shown by proximity to the red 1:1 line. (d) We show this empirical average $A[\beta_{ij}]$ in matrix form (median value for each species pair i, j), to compare with the predicted matrix $E[\beta_{ij}]$ in (b).

parent structure, it conforms to the statistical patterns predicted by our theory. Individual coefficients β_{ij} show a wide dispersion (Fig. 3), which may be widened by inference errors²³. Despite this large spread, when we group interactions involving species with similar relative yields, their average $A[\beta_{ij}|\eta_i, \eta_j]$ lays close to a one-to-one relationship with the theoretical expectation $E[\beta_{ij}|\eta_i, \eta_j]$. The reconstructed statistical pattern in Fig. 3 agrees both qualitatively and quantitatively with the predictions.

This striking agreement between theory and data is quantified for multiple experiments in Fig. 4. We stress that this is a strong test. All results are fully determined by measured abundances, without any adjustable parameter. Furthermore, none of the data used to parameterize theoretical formulas is involved in fitting the empirical interaction coefficients. Finally, we rule out these relationships being artefacts of our method, as they vanish for very sparse or noisy data, and can be violated in simulated ecosystems with a low-dimensional structure, as seen in Fig. 1 and 4.

The approach developed here provides a test of how *typical* an empirical or theoretical interaction network is, given the observed abundances of its species: how similar it is to the majority of possible networks admitting the same equilibrium η_i (Fig. 1). We also detail in Appen-

pendix B an algorithm for generating such typical networks. A deviation from typicality may hint at low dimensional mechanisms, such as particular trade-offs⁴.

We have introduced a novel methodology for thinking about the collective organization of coexistence in ecological communities. This approach goes beyond the particular theoretical predictions (4) and (6), which are simplified results tied to our choice of unstructured prior distribution and linear interactions. When there is a positive but nonlinear relationship between data and predictions, our approach could be improved with more accurate inference and more realistic models, but it already captures an important qualitative feature of community organization. The same methods could be expanded by adding structure to the prior and nonlinearity to the dynamics. This will allow extensions to more complex communities, such as food webs, or networks that have been structured by other ecological and evolutionary processes³². Future work should explore how this approach, based on ideas from statistical physics and generic properties of high-dimensional systems, can be generalized to other biological systems.

Methods

213

Experimental data

214

We employ data from 3 grassland biodiversity experiments in Wageningen, Netherlands²⁹ and Cedar Creek, MN, USA (the Big Biodiversity³¹ and BioCON³⁰ experiments). Each experiment uses a pool of species seeded or planted in various combinations, including some or all possible monocultures ($S = 1$ species), some partial compositions, and all species planted together. We removed the first two year for all experiments as they showed clear evidence of transient dynamics (Appendix C).

Interactions measured in the Wageningen experiment showed much lower inference error than in other experiments. Therefore, we used this experiment to assess our hypothesis that observed abundances are primarily determined by fixed inter-species interactions (Appendix D). The consistency of the equilibrium Lotka-Volterra description (2) was shown through a series of tests: we employed multiple inference procedures for the matrix β_{ij} and carrying capacities K_i , using different subsets of the data for prediction and validation, and found them all statistically significant and in agreement within empirical uncertainty. In particular, carrying capacities K_i inferred from all multispecies plots ($S > 1$) agreed with measurements in monocultures ($S = 1$). Likewise, interactions β_{ij} inferred from all plots with $S < 8$ were consistent with the equilibrium values of $\eta_i = B_i/K_i$ in octoculture ($S = 8$). This strongly supports the simple linear model (2). Interaction estimates from other experiments were less robust and might be affected by nonlinearity, transient dynamics, stochasticity and errors.

Validation of theoretical predictions

244

For each experiment, we first split monoculture ($S = 1$) replicates in two sets, and compute the species' carrying capacities K_i for each set, to be used separately. For a maximal plot biodiversity S_{\max} , all plots with $1 < S < S_{\max}$ and the first set of monocultures were used to infer the interaction matrix β_{ij} using the hyperplane (multilinear) least-squares fit proposed by Xiao et al²³ (see Appendix D). The second set of monocultures and the species abundance B_i in plots with $S = S_{\max}$ were then used to compute the relative yields $\eta_i = B_i/K_i$ in the full community. All calculations were performed 250 times, using different bootstrapped sample means as values for K_i and B_i . Each calculation led to a different set of η_i , β_{ij} and $\bar{\beta}$ (see Appendix A for calculation details).

We tested the two components of the diffuse clique pattern, starting with the pattern of means (4). We plotted the measured values of β_{ij} (hereafter y) against their the-

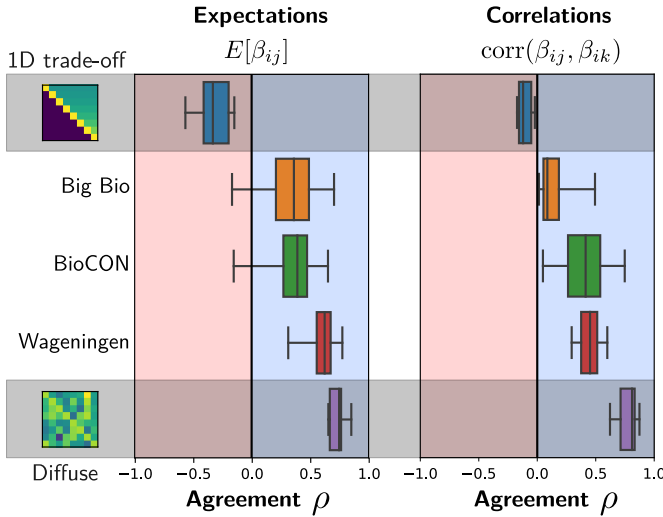


Figure 4: Cross-experiment validation of the two components of the diffuse clique structure. We compute the agreement between the measured and predicted values for: conditional expectations $E[\beta_{ij}|\eta_i, \eta_j]$ (left) and correlations $\text{corr}(\beta_{ij}, \beta_{ik}|\eta_i, \eta_j, \eta_k)$ (right), using the predictions in Fig. 2. We show the agreement metric ρ (see SI Appendix E), comprised between -1 and 1. Boxes and whiskers represent the 50% and 95% CI of bootstrapped values, with the median shown as the center line. The shaded rows show results for two coexistence mechanisms as in Fig. 1: a one-dimensional trade-off with $\rho < 0$ (top row) and our high-dimensional diffuse clique structure with $\rho > 0$ (bottom row), both aggregated over 5 simulated communities with $S = 25$ species. In the Wageningen experiment, ρ is significantly larger than zero for both means and correlations. The Big Bio and BioCON experiments comprise multiple treatments (see SI Appendix E), over which we aggregate to find that zero always lies below the 10th percentile of ρ .

262 theoretical expectation $E[\beta_{ij}|\eta_i, \eta_j]$ (hereafter x). To obtain
263 an empirical estimate of the expectation for a single interaction coefficient, we performed a running average: for
264 each point (x, y) , we replaced its y coordinate by the average \bar{y} within a window centered on x and spanning 10%
265 of the x-axis; we also measure the 90% CI over bootstrapped values (Fig. 3c). We then grouped all values
266 \bar{y} associated with the same species pair (i, j) , took their
267 median, and reconstructed an empirical matrix of expectations B_{ij} (shown in Fig. 3d).

272 To construct a stringent test (see SI Appendix E), the
273 metric of agreement ρ used in Fig. 1 and 4 is defined as the
274 minimum of three correlation scores: ρ_0 testing the over-
275 all relationship between x and \bar{y} , ρ_{row} testing the agree-
276 ment of row-wise trends (within bins of η_i) and ρ_{col} for
277 column-wise trends (within bins of η_j). This ensures that
278 all the qualitative features described in Fig. 2 are present,
279 and reduces the risk of spurious agreement scores.

280 We proceeded similarly to test the pattern of correlations
281 (6). Defining $d_{ij} = \beta_{ij} - E[\beta_{ij}|\eta_i, \eta_j]$, we compute
282 $y = \delta_{jk} - d_{ij}d_{ik}/\text{mean}(d_{mn}^2)$, where $\delta_{jk} = 1$ if $j = k$ and 0
283 otherwise, and the denominator is the sample mean. We
284 then plotted y against the prediction $x = -\eta_j\eta_k/\sum_{l \neq i} \eta_l^2$,
285 performed a running average to get \bar{y} , and constructed an
286 empirical tensor of correlations C_{ijk} from the median of
287 all values associated with each species triplet (i, j, k) .

288 Data availability

289 This study brought together existing data that was ob-
290 tained upon request (Wageningen biodiversity experi-
291 ment data from J. van Ruijven²⁹) and data that is pub-
292 licly available (Big Bio <http://www.cedarcreek.umn.edu/research/data> and BioCON <http://www.biocon.umn.edu/>). Data represented in Fig. 3 and 4 is available
293 at <https://github.com/mrcbarbier/diffuseclique>.

296 Code availability

297 Computer code developed for this study is available at
298 <https://github.com/mrcbarbier/diffuseclique>.

299 Acknowledgments

300 We thank J.-F. Arnoldi, Y. Zelnik and F. Isbell for com-
301 ments. Our gratitude goes to J. van Ruijven for shar-
302 ing data from the Wageningen experiment. Experimental
303 work at Cedar Creek was supported by grants from the
304 US National Science Foundation Long-Term Ecological
305 Research Program (LTER) including DEB-0620652 and
306 DEB-1234162, and further support was provided by the

307 Cedar Creek Ecosystem Science Reserve and the Univer-
308 sity of Minnesota. M.B., C.d.M. and M.L. were supported
309 by the TULIP Laboratory of Excellence (ANR-10-LABX-
310 41) and by the BIOSTASES Advanced Grant, funded
311 by the European Research Council under the European
312 Union's Horizon 2020 research and innovation programme
313 (666971). G.B. was supported by the Israel Science Foun-
314 dation (ISF) Grant no. 773/18.

315 Author contributions

316 G.B. developed the theoretical approach. M.B., G.B. and
317 C.d.M. analyzed the data. M.B. wrote the first draft.
318 All authors contributed substantially to study design and
319 manuscript revisions.

320 References

- [1] Jorge Kurchan and Laurent Laloux. Phase space
321 geometry and slow dynamics. *Journal of Physics A: Mathematical and General*, 29(9):1929, 1996.
322
- [2] Mikhail Tikhonov and Remi Monasson. Innovation
323 rather than improvement: a solvable high-dimensional
324 model highlights the limitations of scalar fitness. *Journal of Statistical Physics*, pages
325 1–31, 2018.
326
- [3] James S Clark, Mike Dietze, Sukhendu Chakraborty,
327 Pankaj K Agarwal, Ines Ibanez, Shannon LaDeau,
328 and Mike Wolosin. Resolving the biodiversity para-
329 dox. *Ecology Letters*, 10(8):647–659, 2007.
330
- [4] Adam Thomas Clark, Clarence Lehman, and David
331 Tilman. Identifying mechanisms that structure eco-
332 logical communities by snapping model parameters
333 to empirically observed tradeoffs. *Ecology letters*,
334 21(4):494–505, 2018.
335
- [5] Robert M May. Will a large complex system be sta-
336 ble? *Nature*, 238:413–414, 1972.
337
- [6] Matthieu Barbier, Jean-François Arnoldi, Guy
338 Bunin, and Michel Loreau. Generic assembly pat-
339 terns in complex ecological communities. *Proceedings
340 of the National Academy of Sciences*, 115(9):2156–
341 2161, 2018.
342
- [7] GF Gause. The struggle for existence. *Williams and
343 Wilkins, Baltimore*, 1934.
344
- [8] David Tilman. *Resource competition and community
345 structure*. Princeton University Press, 1982.
346

349 [9] Michel Loreau. *From populations to ecosystems: 395
350 Theoretical foundations for a new ecological synthesis* (MPB-46). Princeton University Press, 2010. 396
351

352 [10] Robert MacArthur. Species packing, and what 397
353 competition minimizes. *Proceedings of the National 398
354 Academy of Sciences*, 64(4):1369–1371, 1969. 399

355 [11] Simon A Levin. Community equilibria and stability, 400
356 and an extension of the competitive exclusion principle. 401
357 *The American Naturalist*, 104(939):413–423, 402
358 1970. 403

359 [12] Peter Chesson. Quantifying and testing coexistence 404
360 mechanisms arising from recruitment fluctuations. 405
361 *Theoretical population biology*, 64(3):345–357, 2003. 406

362 [13] György Barabás, Rafael D’Andrea, and Simon Mac- 407
363 cracken Stump. Chesson’s coexistence theory. *Eco- 408
364 logical Monographs*, 2018. 409

365 [14] Benoît Jaillard, Camille Richon, Philippe Deleporte, 410
366 Michel Loreau, and Cyrille Viole. An a posteriori 411
367 species clustering for quantifying the effects of 412
368 species interactions on ecosystem functioning. *Methods 413
369 in Ecology and Evolution*, 9(3):704–715, 2018. 414

370 [15] Eugene P Wigner. On the distribution of the roots of 415
371 certain symmetric matrices. *Annals of Mathematics*, 416
372 pages 325–327, 1958. 417

373 [16] Philip W Anderson. Absence of diffusion in certain 418
374 random lattices. *Physical review*, 109(5):1492, 1958. 419

375 [17] Serguei Saavedra, Rudolf P Rohr, Jordi Bascompte, 420
376 Oscar Godoy, Nathan JB Kraft, and Jonathan M 421
377 Levine. A structural approach for understanding 422
378 multispecies coexistence. *Ecological Monographs*, 423
379 87(3):470–486, 2017. 424

380 [18] Richard Levins and David Culver. Regional 425
381 coexistence of species and competition between rare 426
382 species. *Proceedings of the National Academy of 427
383 Sciences*, 68(6):1246–1248, 1971. 428

384 [19] David Tilman. Competition and biodiversity in 429
385 spatially structured habitats. *Ecology*, 75(1):2–16, 1994. 430

386 [20] Guy Bunin. Interaction patterns and diversity in 431
387 assembled ecological communities. *arXiv preprint 432
388 arXiv:1607.04734*, 2016. 433

389 [21] Claire Mazancourt, Forest Isbell, Allen Larocque, 434
390 Frank Berendse, Enrica Luca, James B Grace, Bart 435
391 Haegeman, H Wayne Polley, Christiane Roscher, 436
392 Bernhard Schmid, et al. Predicting ecosystem 437
393 stability from community composition and biodiversity. 438
394 *Ecology letters*, 16(5):617–625, 2013. 439

395 [22] Charles K Fisher and Pankaj Mehta. Identifying 440
396 keystone species in the human gut microbiome from 441
397 metagenomic timeseries using sparse linear regres- 442
398 sion. *PloS one*, 9(7):e102451, 2014. 443

399 [23] Yandong Xiao, Marco Túlio Angulo, Jonathan Fried- 400
400 man, Matthew K Waldor, Scott T Weiss, and Yang- 401
401 Yu Liu. Mapping the ecological networks of microbial 402
402 communities. *Nature communications*, 8(1):2042, 403
403 2017. 404

404 [24] Daniel S Maynard, J Timothy Wootton, Carlos A 405
405 Serván, and Stefano Allesina. Reconciling empirical 406
406 interactions and species coexistence. *Ecology letters*, 407
407 2019. 408

408 [25] Daniel S Maynard, Zachary R Miller, and Stefano 409
409 Allesina. Predicting coexistence in experimental eco- 410
410 logical communities. *bioRxiv*, page 598326, 2019. 411

411 [26] Hugo Fort. Quantitative predictions from competi- 412
412 tion theory with an incomplete knowledge of model 413
413 parameters tested against experiments across diverse 414
414 taxa. *Ecological Modelling*, 368:104–110, 2018. 415

415 [27] Edwin T Jaynes. On the rationale of maximum- 416
416 entropy methods. *Proceedings of the IEEE*, 417
417 70(9):939–952, 1982. 418

418 [28] Frédéric Vrins. Sampling the multivariate stan- 419
419 dard normal distribution under a weighted sum 420
420 constraint. *Risks*, 6(3):64, 2018. 421

421 [29] Jasper Van Ruijven and Frank Berendse. Long-term 422
422 persistence of a positive plant diversity–productivity 423
423 relationship in the absence of legumes. *Oikos*, 424
424 118(1):101–106, 2009. 425

425 [30] Peter B Reich, David Tilman, Shahid Naeem, 426
426 David S Ellsworth, Johannes Knops, Joseph Craine, 427
427 David Wedin, and Jared Trost. Species and 428
428 functional group diversity independently influence 429
429 biomass accumulation and its response to CO₂ and 430
430 N. *Proceedings of the National Academy of Sciences*, 431
431 101(27):10101–10106, 2004. 432

432 [31] David Tilman, Peter B Reich, and Johannes MH 433
433 Knops. Biodiversity and ecosystem stability in 434
434 a decade-long grassland experiment. *Nature*, 435
435 441(7093):629, 2006. 436

436 [32] Sergi Valverde, Jordi Piñero, Bernat Corominas- 437
437 Murtra, Jose Montoya, Lucas Joppa, and Ricard 438
438 Solé. The architecture of mutualistic networks as an 439
439 evolutionary spandrel. *Nature ecology & evolution*, 440
440 2(1):94, 2018. 441